

METHODOLOGY FOR AERODYNAMIC DESIGN AND OPTIMIZATION OF AXIAL ROTOR BLADE BASED ON THE EFFECTS OF SWEEP AND DIHEDRAL

R. G. RAMIREZ CAMACHO, A. A. OLIVEIRA, W. OLIVEIRA, E. R. SILVA.

Universidade Federal de Itajubá -UNIFEI
Instituto de Engenharia Mecânica
Av. BPS Nº 1.303, Itajubá, MG Brasil.

ramirez@unifei.edu.br, waldir@unifei.edu.br, Edna@yahoo.com.br

ABSTRACT

This work presents a methodology for aerodynamic design of axial flow pump rotors based on initial values established. This methodology proposes a modification next to the blade tip region, in order to minimize the effects caused by the spacing between the blade tip and the casing (tip clearance) in the flow of axial flow rotors. One is the displacement of the blade profiles near to the blade tip region. These displacements are known as sweep and dihedral. An axial flow pump rotor was designed and a certain tip clearance was fixed. This conventional rotor was then modified and applied the sweep and dihedral in the region near to the blade tip. By means of techniques of computational fluid dynamics (CFD), the search for the optimal value of efficiency was made through the CRSA optimizer with Fortran platform that manages the system of mesh generation with the numerical simulation software, FLUENT ®. Based on the optimal values found, a restriction of range of sweep and dihedral was performed in order to obtain a more accurate optimal value. Having found the best value, i. e., the highest efficiency, was compared to the original design (conventional rotor), for a range of flow rate. A real gain was observed across the range analyzed, showing the effectiveness of the application of sweep and dihedral.

Keywords: Axial Flow Pump, Aerodynamic Design, Sweep, Dihedral, Optimization, CRSA, CFD

1 INTRODUCTION

Due to necessity and interests over the environment, that have the different nations, about natural sources preservation and the decrease on environment impact for the maintenance of a sustainable development in this matter, different governments and industries that are focused in the hydropower sector generation, have being developed researches about diverse designs for a fish friendly turbine, according with the project requirements that are dependent to the operations conditions existents like the hydraulic heads, the flow capacity among others, to without have a significative reduction on the efficiency in the power generation.

Currently there are numerous turbines operating with high, medium and low hydraulic heads with high efficiencies, many of which cause environmental damages, especially about the injuries caused to the fishes. In this sense it is important, a hydraulic turbine rotors design project, that can reach environmental criteria and standards.

Having the preliminary axial rotor's hydrodynamic design, improvements can be made (modifications) in the geometry of the blades (retaining the diameters of the tip and the blade root) for a certain top clearance. For those conditions, resulting from the modification of the axial rotor blades geometry, the main objective is to minimize flow losses coming from the top clearance and therefore maximize the rotor's hydraulic efficiency.

There are some techniques aimed at modifying the blade's geometry and are applied either in the closest region to the blade tip or even on top of blade (Silva, 2012). Those techniques have the main

purpose to reduce effects caused by top clearance in axial turbomachines. Among these techniques, can be mentioned: 1) pressure side squealer tip and/ or suction side squealer tip of the blade, which can be total (the whole extension of the sides of pressure and / or suction) or partial (in some parts of sides suction and / or pressure). The squealer tip is applied only on the top of blade, for example, Camci *et al.* (2003); 2) extension top of blade (tip platform extension) that can be applied on the pressure side or suction side of blade, can be total (in the entire length of the sides of pressure or suction) or partial (in some parts of the suction or pressure side), for example, Camci and Dey (2004); 3) profile displacement along its chord (sweep) and / or profile displacement perpendicularly to its chord (dihedral). These displacements can be applied in a closer region the blade tip or extend in a more distal region of the blade tip.

The literature review about clearance top and sweep and dihedral by Lakshminarayana (1996) is the main textbook for the development of this research. The author discusses in detail various topics of interest in turbomachines, among them stand out the mechanism of the losses in turbomachines, including losses from the top and the effects of clearance-top on their performance. Presents several loss correlations developed by him and other authors. Discusses in detail the equations governing the flow in turbomachines and provides an excellent contribution on the most appropriate turbulence models for flows in turbomachines.

Kwedikha (2009) presents a comparison of two cases with application of combined effects of sweep and dihedral in the blades, considering industrial examples. The author shows that even applied near the blade tip, end up influencing the flow in regions of the channels inside the blade. Smith and Yeh (1963) present an approximate method to include sweep and dihedral in the design of axial turbomachines. They also present an analytical method for the correction in the blade tip region.

Vad (2008) presents non-radial stacking techniques (with displacement profiles) of the blade sections for axial fans and compressors in the design flow. Suggests the application of sweep and dihedral to improve the total efficiency and increase the operating range of stall in axial fans and compressors. The author emphasizes the fundamental role of the computational fluid dynamics (CFD) in the evaluation of the aerodynamic effects of non-radial stacking the blades profiles as well as the incorporation of sweep and dihedral in the systematic design techniques of axial turbomachines blades

In this work, just the sweep and dihedral are analyzed (without combinations with the two other modification techniques described above) and applied to a small region near the tip of blade. Those two types of displacement are applied simultaneously.

The existing literature basically reports the project of conventional axial turbomachines that supply energy to fluid (without sweep and dihedral), such as pumps and fans. Apparently there isn't a design methodology able to provide a general procedure for the design of axial pumps with sweep and / or dihedral.

The hydrodynamic performance characteristics of axial pumps, besides the rotation and flow rate, depends greatly on the rotor geometry, particularly their blades. For a given geometry of the blades, both the pump head and its stability margin are influenced by variation in clearance top. Similarly, for a given top clearance, pump head and the flow rate are influenced by the variation in geometry of the blades.

It is presented below the most relevant papers about the design conventional axial rotor used in this research. The axial rotor design is based on the research of Bran and Souza (1969) who present a similar procedure that of Pfleiderer (1960). They applied the wing lift theory to the aerodynamic

design of axial rotors for pumps, fans and turbines and showed computations examples for rotors. The paper provides some charts that are important for the preliminary design of axial rotors. Macintyre (1980) also presents the wing lift theory applied to axial rotors, but presents no example calculation. Wallis (1983) presents a rather complete theory for the design of both rotors and stators (before and after the rotor) of axial fans based on the cascade theory. Wallis presents several calculation examples for axial rotors, using both the condition of free vortex as the forced vortex.

In available technical literature, there are few publications related to the influence of sweep and dihedral in hydraulic turbomachines, specifically in axial pumps. Basically, these works are exclusive of leading multinational companies, thus making it difficult to obtain specific information about the research topic.

2 MATHEMATICAL MODEL AND TURBULENCIA

Turbulent flows are characterized by, which carry quantities of mass, momentum, scalar species that fluctuate in time and space not permanent, irregular movements. Velocities and fluid properties commonly exhibit random variations at different scales of specter.

2.1 Equations for the Turbulent Flow

The FLUENT ® program uses the Reynolds equations (RANS - Reynolds-averaged Navier-Stokes) for solving problems of turbulent flow. In this technique, all dependent variable, scalar or vector can be decomposed in an average time of over a fluctuating part which when introduced into the conservation equations in non-inertial systems results.

Equation of conservation of mass:

$$\frac{\partial}{\partial x_i}(\bar{w}_i) = 0 \quad (1)$$

Equation of conservation of momentum:

Considering the apparent acceleration, \bar{a}_{apar} , for stationary turbomachinery, $\ddot{\vec{R}}_0 = 0$, with constant angular velocity $\dot{\omega} = 0$, is reduced to.

$$\bar{a}_{apar} = 2\vec{\omega} \times \vec{w} + \vec{\omega} \times (\vec{\omega} \times \vec{r}_p) \quad (2)$$

Therefore, considering permanent flow relative to a non-inertial system, we obtain the equation of conservation of momentum given by Reynolds averaged.

$$\rho \bar{w}_j \frac{\partial \bar{w}_i}{\partial x_j} + \rho (\bar{a}_{apar})_i = -\frac{\partial \bar{p}}{\partial x_i} + \mu \frac{\partial^2 \bar{w}_i}{\partial x_j^2} - \rho \frac{\partial}{\partial x_j} \overline{w'_i w'_j} + \rho \bar{g} \quad (3)$$

Generally, the turbulent part and the viscous stress are grouped. Thus, the general or overall tension is (Viçosa, 2004) represented by:

$$\tau_{g_{ij}} = -\overline{\rho w'_i w'_j} + \mu \left(\frac{\partial \bar{w}_i}{\partial x_j} + \frac{\partial \bar{w}_j}{\partial x_i} \right) \quad (5)$$

The Reynolds tensor can be appropriately modeled using the Boussinesq hypothesis, represented in terms of a turbulent viscosity.

The Reynolds tensor τ_i can be appropriately modeled using the Boussinesq hypothesis, represented in terms of a turbulent viscosity μ_t .

$$-\rho \overline{w'_i w'_j} = \mu_t \left(\frac{\partial w_i}{\partial x_j} + \frac{\partial w_j}{\partial x_i} \right) - \frac{2}{3} \left(\rho k + \mu_t \frac{\partial w_k}{\partial x_k} \right) \delta_{ij} \quad (6)$$

where k is the turbulent kinetic energy and δ_{ij} is the Kronecker delta operator.

In this work, the turbulent viscosity μ_t is obtained using the standard $k-\omega$ SST turbulence, which uses the Boussinesq hypothesis.

2.2 $k-\omega$ SST Model

The choice of model depends on the type of analysis. In this work, the $k-\omega$ SST turbulence model is used. This model was developed by Menter (1993) to effectively combine the robust and accurate formulation of the model $k-\omega$ in regions near to the wall, with the advantages of $k-\epsilon$, free to treat runoff. Its formulation is similar to the model $k-\omega$ but includes certain considerations. O model $k-\omega$ standard and $k-\epsilon$ are both multiplied by a function. This function takes the value of 1 in regions near to the wall, activating the model $k-\omega$; and the value of 0, when tested in a region away from the wall, intervening here $k-\epsilon$ model. The constants of the model $k-\omega$ SST, differ from those in the model $k-\omega$. These features make the model $k-\omega$ SST more accurate and reliable for a wider range of flows, such as problems in regimes with adverse pressure gradients and separation of the boundary layer (ANSYS, Inc., 2011). The $k-\omega$ model uses wall functions, allowing adopt the value of Y plus 200 to 400.

3 NUMERICAL SIMULATION

The calculation of the axial flow rotor, based on the pre-preliminary design was performed by commercial software FLUENT ®. The following hypotheses were considered: relative flow permanent, incompressible and isothermal regime. The bulk density and the dynamic viscosity of water was; $\rho = 998.2 \text{ kg/m}^3$ and $\mu = 0.001003 \text{ kg / m-s}$ respectively.

3.1 Geometry and Mesh

The rotor geometry was generated through editing a script command in Tcl / Tk language for interpretation by the ICFM-CFD ® software, the script is based on a text file with executable commands for generating points, curves, surfaces and parameters mesh (script.rpl). In this, they are given basic dimensions of information obtained from the preliminary design of axial rotor, such as: number of blades, 4; inner diameter of 920 [mm]; outer diameter, 1700 [mm]; number of hub stations until the blade tip, 10; chord length of each profile; refinement coefficient of each profile; stagger angle of each profile; points of each profile coordinates; value of clearance in the blade tip, 8.5 [mm]; sweep and dihedral displacements [mm]; $n = 310 \text{ rpm}$.

After creating the geometry (Fig. 1), are edited in script commands with parameter data mesh on different surfaces: cube, top, pressure, suction, trailing edge, leading edge, etc). The mesh used was unstructured type with tetrahedral, prismatic and pyramidal elements. In Figure 1, we observe the

mesh refinement in regions of the top and leading - trailing edges. The refinement in these regions is important due to the high pressure gradients; velocity and turbulent kinetic energy are present.

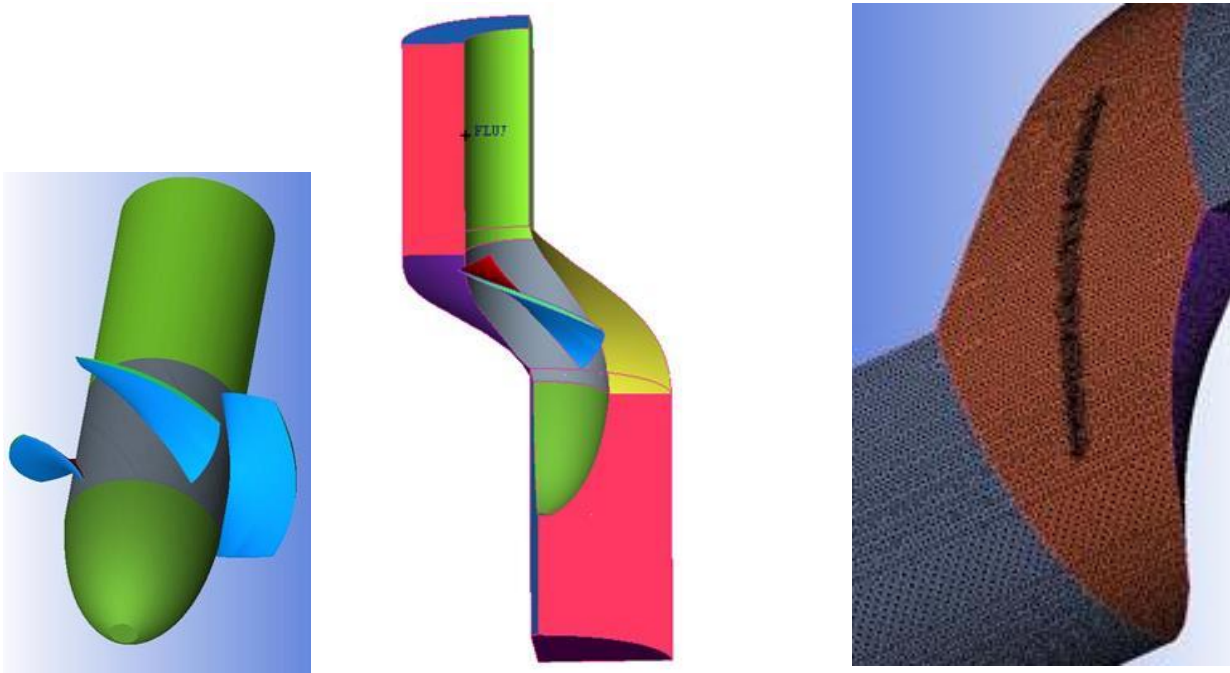


Figure 1 - Geometry and mesh, number of elements in the rotor channel: 2.244.928.

3.2 Boundary Conditions

Input surface: This surface velocity condition was set at the input (velocity-inlet), which was specified initial gauge pressure and flow rate. According to the preliminary design, was considered a gauge static pressure at the inlet of 58305 Pascal, and a volumetric flow rate 3063.86 kg/s, with low levels of turbulence (5%).
Exit surface: This surface was used the pressure condition at the outlet (pressure-outlet). The pressure was established out of 124367 Pascal according to the rotor design based on the study of pump cavitation.

3.3 Discretization and Interpolation Schemes

P For incompressible flows, an algorithm must be used to obtain the fields of pressure and speed. In this work we used the SIMPLE algorithm (Semi-Implicit Method for Pressure-Linked Equations), where there is an iterative process based on the relation between velocity and pressure corrections, thereby strengthening the conservation of mass and then obtaining the pressure field. For the numerical solution of the equations of momentum, turbulent kinetic energy and specific dissipation rate, the second-order scheme (Second order Upwind) is used.

4 METHODOLOGY OF INTEGRATION PROCESS

For the optimization procedure the global optimization strategies algorithm known as stochastic Controlled Random Search Algorithm CRSA, which is based an initial population and promotes

iterative substitutions of the worst individuals was used by the best, wishing that the population will contract up around the global optimum. In the design variables to be optimized, defined as the sweep and dihedral displacements were introduced. For the solution of the flow in the rotor used the FLUENT® software, in which the boundary conditions, turbulence model (k- ω -SST), thermodynamic properties, rotation and convergence criteria of the solution, were introduced through auxiliary files journal.jou type. The assembler program or process manager is the optimization algorithm written in FORTRAN language CRSA, which allows you to manage the integration through DOS commands executed internally in the program (command iqsystem) this way you can run inside the ICEM-CFD and FLUENT software with its auxiliary files; script.rpl and journal.jou. (Fig 2)

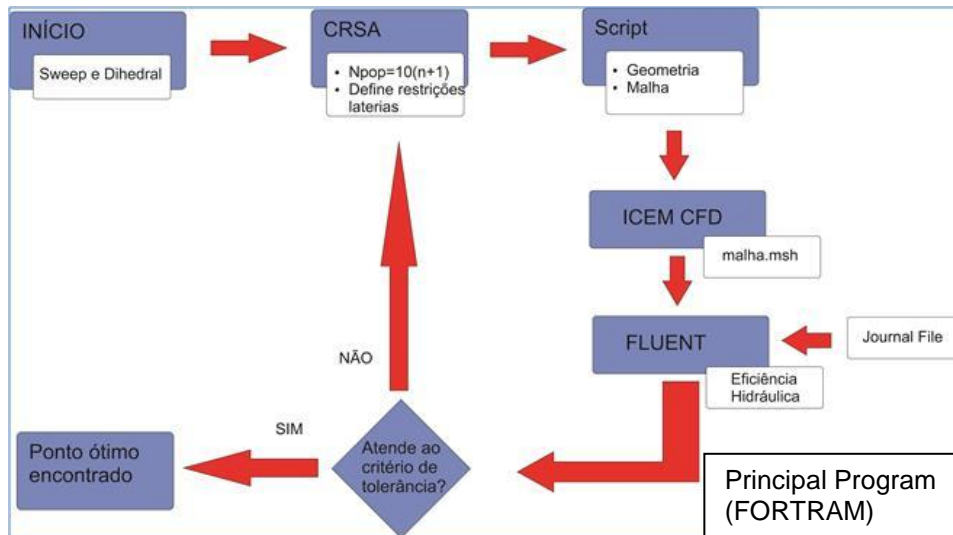


Figure 2 - Flowchart of process integration (Silva 2011)

Following the flowchart described in Fig 2, we define the limits of design variables in the CRSA, as well as the size of the experimental plan. And then based on this script.rpl is edited and executed by ICEM-CFD® on BACH (hidden) mode, generating the new geometry and the malha.msh file. The FLUENT® software through journal.jou file reads the new mesh and introduces the boundary conditions, methods of calculation, convergence criteria, among others. After achieving the residue $\epsilon = 10^{-4}$ in CFD simulation, it generates a text file that contains the value of the axial pump hydraulic efficiency. This value is obtained by means of tool called turbotopology / FLUENT®.

This work was carried out small variations in the blade tip, and the sweep [-40 mm +40 mm] and dihedral [-20 to +20 mm] mm. (Fig 3). Another important parameter to be set initial, was the size of the experimental plan, with $NPOP = 10(n + 1)$, where n is the number of variables in the problem. Given the two variables, sweep and dihedral, ($n = 2$) we obtain, for example a plan of experiments with 30 random variations of sweep and dihedral.

After the generation of the plan of experiments, the values of hydraulic efficiencies of all points of the DOE (Desing of experiment) are obtained, then the CRSA starts the optimization process searching for a maximum hydraulic efficiency. This process can take a few hours to a few days depending on the number of mesh elements and the complexity of the solution. The introduction of the diffuser would increase the time to calculate the flow in the pump considerably.

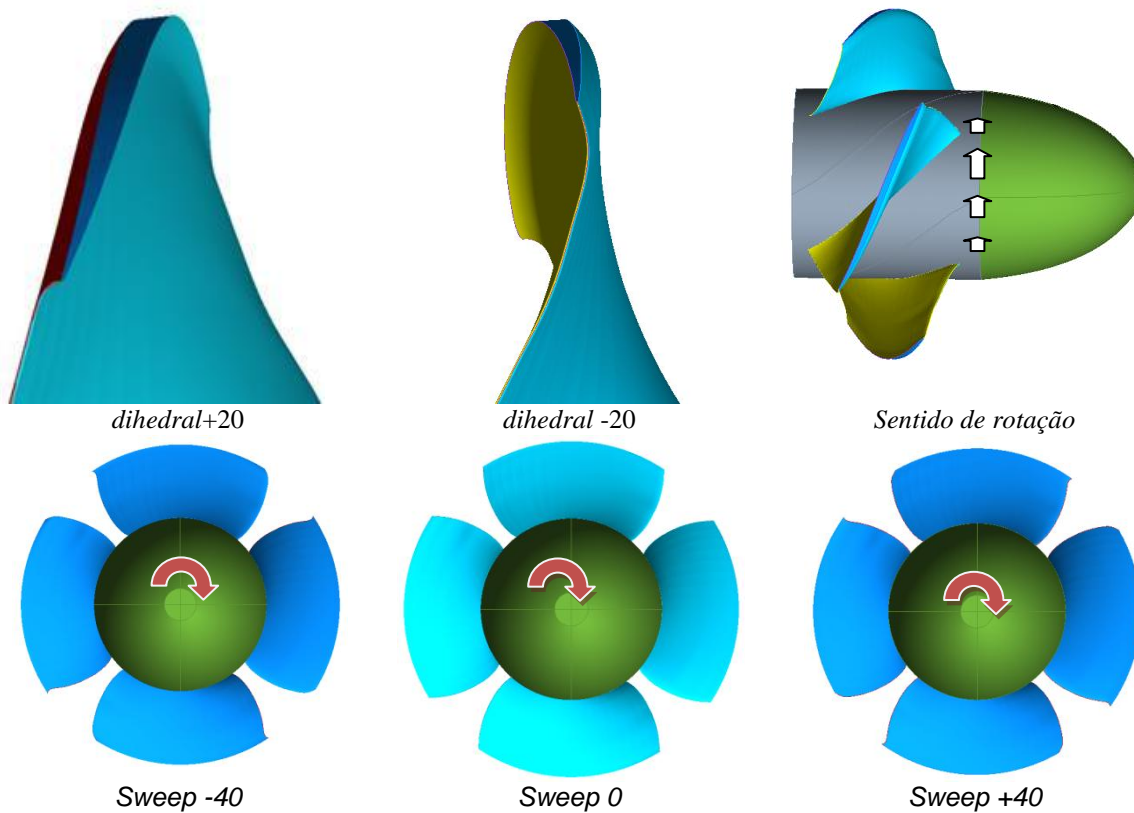


Figure 3 - Limits on variations of displacement sweep and dihedral

5 HYDRAULIC EFFICIENCY

In a first approach, an initial population was generated 30 random points for the design variables, with lateral limits of the -40mm +40 mm for the sweep and -20mm to +20 mm for the dihedral, 100 trials being set for the search optimal objective function, hydraulic efficiency.

Figure 5 shows on the ordinate axis of the dihedral and sweep in axis of abscissa and hydraulic efficiency in z-axis (3D). It has been found that there is a high concentration in the negative sweep and dihedral in so far that the CRSA will population for contracting an overall maximum efficiency (Fig. 5).

In a second approach, a contraction of the population varying limits of sweep and dihedral [0 -40] and [-20 0] respectively was taken with the aim of make a more debugged search of the hydraulic efficiency. In Figure 6, show the new values of hydraulic efficiency with the new limits of sweep and dihedral variation.

This analysis found the value of the maximum hydraulic efficiency 85.98%, for the values of sweep and dihedral = -18.2 mm = -7.5 mm. Figure 7 shows the optimal sweep and dihedral displacements to obtain the maximum efficiency. It should be noted that variations in the blade tip are small while maintaining the integrity of the preliminary design. This methodology is addressed with technological objective, to provide information for improving the design hydraulic pumps.

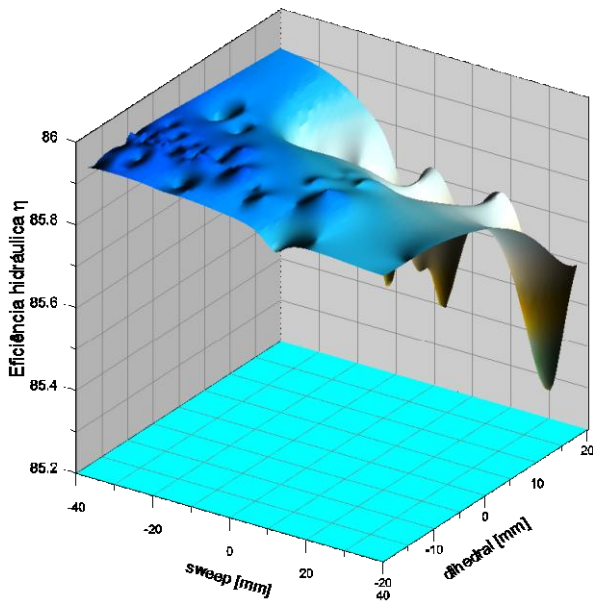


Figure 5- Process optimization, initial population 30, 100 attempts to search.

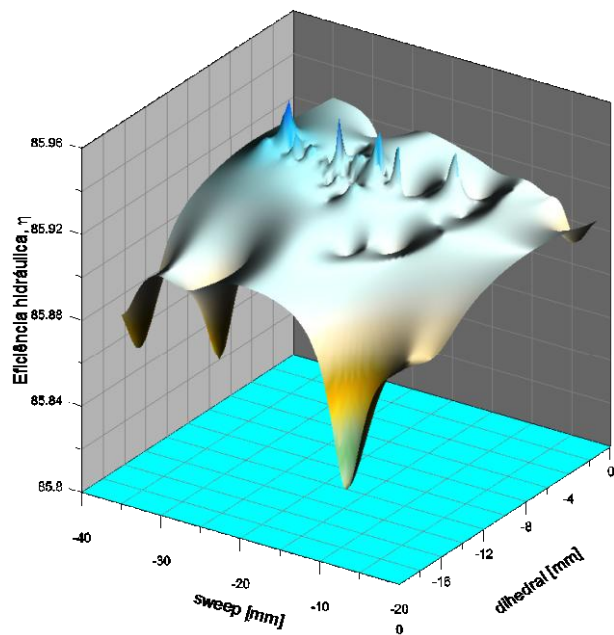


Figura 6- Process optimization, initial population 30, 50 attempts to search.

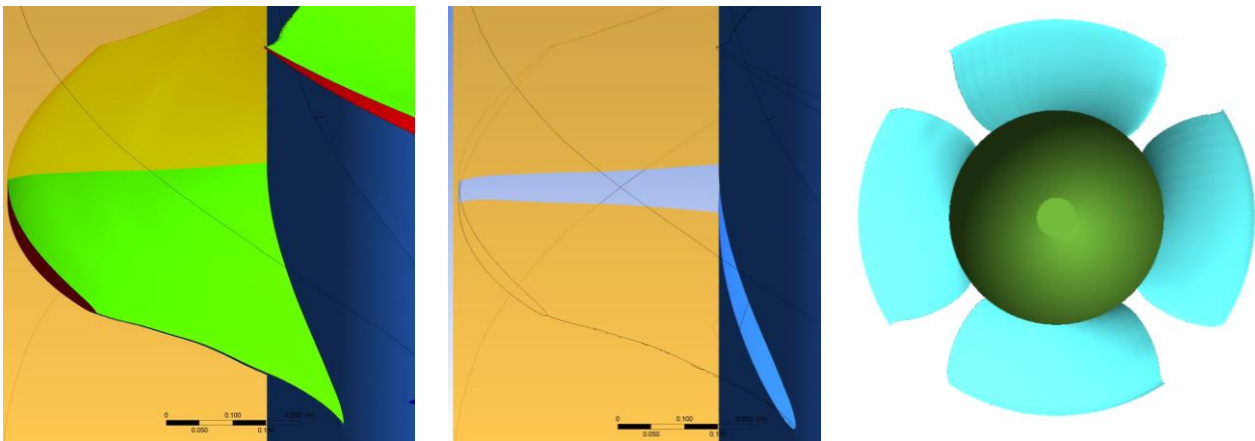


Figure 7 - Geometry of optimum blade: $sweep = -18.2\text{mm}$ e $dihedral = -7.5\text{mm}$

Figure 8 shows the curve H, shaft power, hydraulic power and efficiency for 106 different flow rates. To find that in the whole range of flows, the optimized rotor provided the best efficiencies compared to the original design, ie, without any adjustment for the effects of displacement sweep or dihedral. Moreover, we note that the maximum efficiency of both the optimized rotor as the original rotor are around $3.52 \text{ m}^3 / \text{s}$. Clearly there is a difference between the flow obtained from the CFD calculation and design flow of $7.03 \text{ m}^3 / \text{s}$ is necessary to make corrections to the preliminary design. Note that the flow shown in the curves represents only a quarter of the total flow.

On the other hand, to have a final definition of the efficiency curve is necessary to make the experimental validation, in order to quantify the effects caused by hydraulic losses, but also the effects of cavitation. In the performance curve reported by CFD simulation for optimum rotor with maximum efficiency of 85.6% at a flow rate of $3.74 \text{ m}^3 / \text{s}$, exceeding flow of $3.0 \text{ m}^3 / \text{s}$. determined in preliminary design of axial pump, this occurrence can be explained by introducing the viscous and the tip off, the CFD calculation purposes.

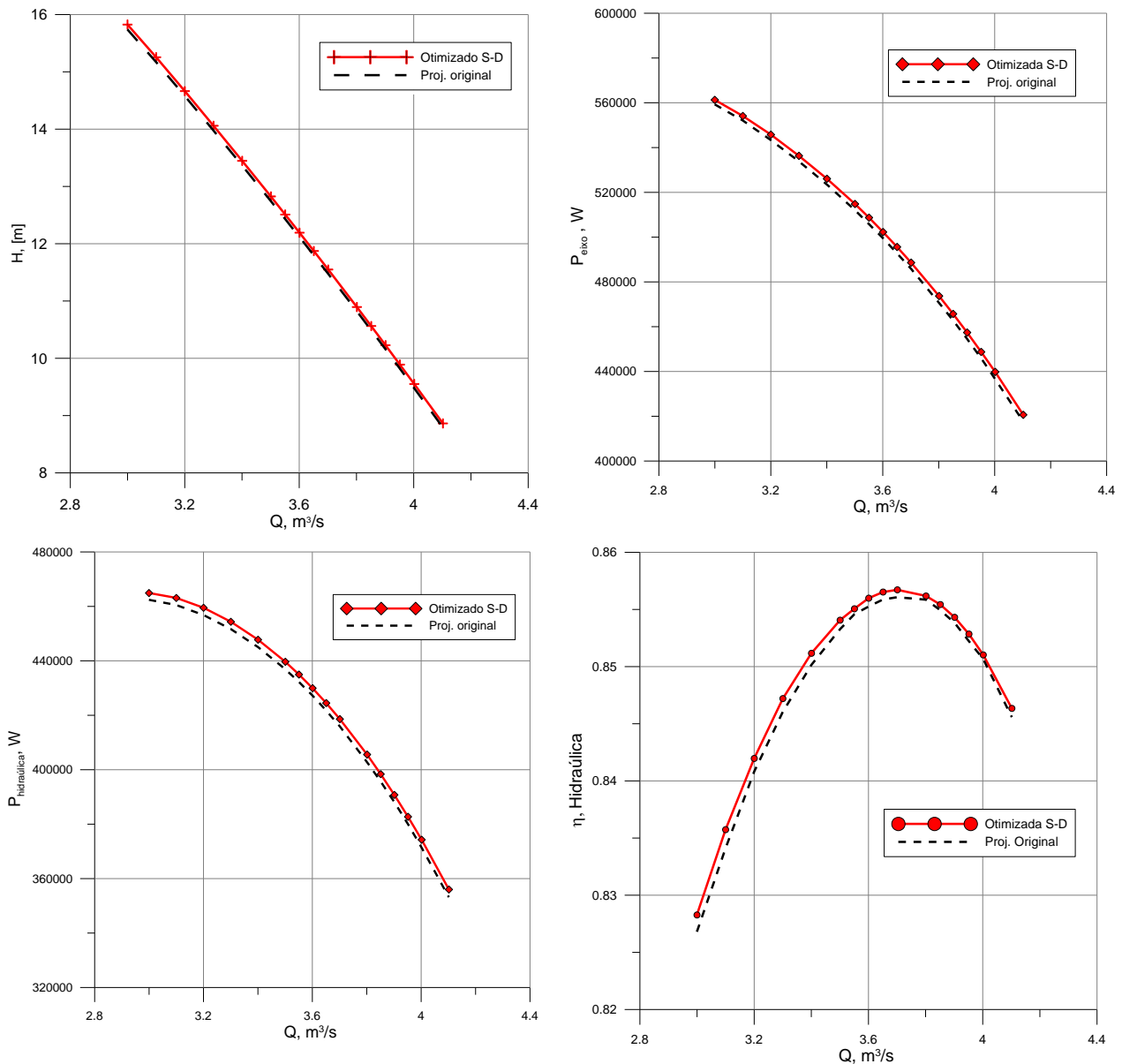


Figure 8 - Characteristic curves Head, P_{shaft} , $P_{hidraulics}$ and hydraulic efficiency

6 CAVITATION

Cavitation analysis using CFD post-processing tools based on the pressure fields are very useful for quantifying the formation of cavitation regions. A way of analysis is mapping the vapor pressure of 2346 Pas water through the generation of iso surfaces with a value of 2346 Pas throughout the computational domain rotor. Therefore you can define how the cavitation region given by the ratio between the surface of cavitation about the rotor area (warhead, cube and shovel). In Figure 9, the ratio $(A_c/A_{p\acute{a}})100$ in order to quantify the intensity of cavitation, in which the minimum values of cavitation are found not at maximum efficiency, however around 72% is presented. For flow below the nominal, cavitation enters an unstable region around 9-10 m^3/s . Is worth noting that the flow shown in the cavitation curves represents the total flow.

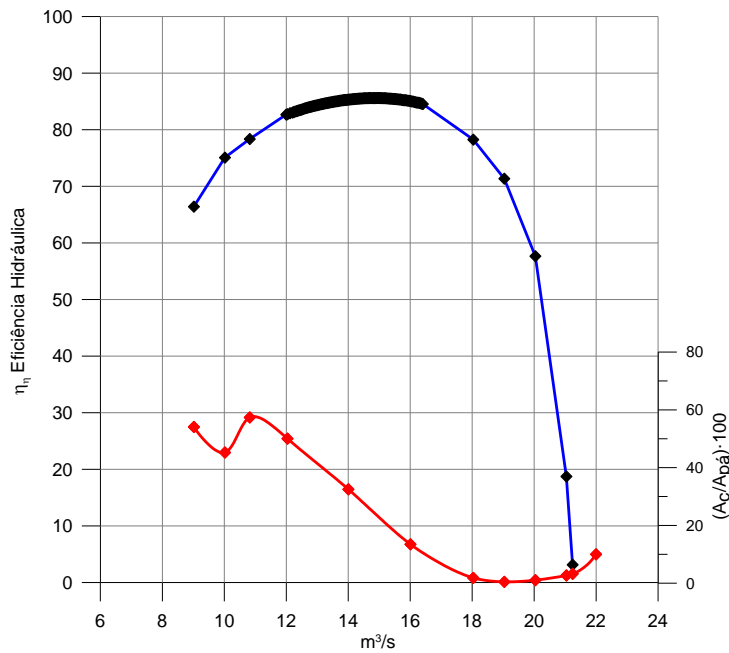


Figure 9 - Hydraulic efficiency and cavitation intensity depending on the volumetric flow

As shown in Fig 9, the minimum cavitation corresponds with efficiencies around 72%. However, the value of the maximum efficiency value corresponds to 15% of the intensity of cavitation. This behavior is common in pumps since they the rotors operate at maximum hydrodynamic loading to attain maximum efficiencies.

Importantly, further consideration of cavitation can be performed using models for multiphase flows, in which are expected phase changes, aiming to more realistically characterize the phenomenon of cavitation. However this approach requires a greater computational cost when integrated with optimization algorithms. On the other hand the monophasic analysis of cavitation models by mapping the vapor pressure of the liquid operated by the turbomachinery has been shown to be suitable for analyzes in several rotors of pumps and turbines in the industry.

7 CONCLUSION

Have been presented and analyzed the results obtained of the numerical simulation using techniques of computational fluid dynamics CFD. The simulations were performed for both conventional axial rotor as for the modified through the effects of sweep and dihedral rotor. Methodologies for Automatic generation of geometry and mesh were presented as well as the iteration between numerical simulation software with the CRSA optimizer. Two approaches aiming to determine the optimum sweep and dihedral values that correspond to the maximum efficiency were carried out.

The numerical results showed that the application of sweep and dihedral contributed to an increase in hydraulic efficiency of the axial rotor across the range of flow rates examined, even if that application were performed in only a small region near the blade tip, corresponding to only 10 % of the blade height in order to maintain the integrity of the preliminary design.

REFERENCES

1. SILVA, L. M. 2012, Cálculo do Escoamento em uma Turbina Axial de Alta Pressão com Diferentes Configurações na Geometria do Topo do Rotor Utilizando Técnicas de CFD, Dissertação de Mestrado em Aerodinâmica, Propulsão e Energia, Instituto Tecnológico de Aeronáutica – ITA, São José dos Campos - SP, 180 p.
2. CAMCI, C., DEY, D. KAVURMACIOGLU, L. 2003, Tip Leakage Flows Near Partial Squealer Rims in an Axial Flow Turbine Stage, GT2003-38979, IGTI/ASME TURBO EXPO 2003, June 2003, Atlanta, Georgia, 1-12 pp.
3. DEY, D., CAMCI, C. 2004, Tip Desensitization of an Axial Turbine Rotor Using Tip Platform Extensions, von Karman Institute Lecture Series VKI-LS 2004-02, Turbine Blade Tip Design and Tip Clearance Treatment, 19-23 January 2004, pp. 42-62, ISBN 2-930389-51-6, Brussels, Belgium Paper 2001-GT-0484, ASME International Gas Turbine Conference
4. LAKSHMINARAYANA, B., 1996, Fluid Dynamics and Heat Transfer of Turbomachinery, John Wiley & Sons, Inc. 820 pp.
5. KWEDIKHA, A. R. 2009, Aerodynamic Effects of Blade Sweep and Skew Applied to Rotors of Axial Flow Turbomachinery, Doctor of Philosophy Thesis, University of Technology and Economics, Budapest, Hungary, 102 pp.
6. SMITH, L. M., YEH, H. 1963, Sweep and Dihedral Effects in Axial-Flow Turbomachinery, Journal of Basic Engineering, Transactions of the ASME, Vol. 85, pp. 401-416
7. VAD, J. 2008, Aerodynamic Effects of Blade Sweep and Skew in Low-Speed Axial Flow Rotors at the Design Flow Rate: An Overview”, Proceedings of the Institution of Mechanical Engineers A, Vol. 222, Nr. 1, pp. 69-85.
8. BRAN, R., SOUZA, Z. 1969, Máquinas de Fluxo: Bombas, Ventiladores e Turbinas, Ao Livro Técnico S. A., 345 p.
9. PFLEIDERER, C. 1960, Bombas Centrífugas y Turbocompresores, Editorial Labor S. A., 631 p.
10. MACINTYRE, A. J. 1980, Bombas e Instalações de Bombeamento, Editora Guanabara Dois S.A., 667 p.
11. WALLIS, R. 1983, Axial Flow Fans and Ducts, John Wiley & Sons, Inc., 478 pp.
12. MENTER, R. F. 1993, Zonal Two-Equation Kappa-Omega Turbulence Models for Aerodynamic Flows, Fluid Dynamics Conference, Orlando, U.S.A.
13. ANSYS INC. 2011, ANSYS FLUENT Theory Guide, U.S.A.
14. SILVA, E. R. 2011, Técnicas de Metamodelagem Aplicadas à Otimização De Turbomáquinas, Tese de Doutorado em Engenharia Mecânica, Universidade Federal de Itajubá, Itajubá - MG, 141 p.